Modeling graphene-based nanoelectromechanical devices

M. Poetschke,[1] C. G. Rocha,[1] L. E. F. Foa Torres,[2] S. Roche,[1,3,4] and G. Cuniberti[1]
[1]*Institute for Materials Science and Max Bergmann Center of Biomaterials, Dresden University of Technology, D-01062 Dresden, Germany*
[2]*Instituto de Física Enrique Gaviola (CONICET) and FaMAF, Universidad Nacional de Córdoba, Ciudad Universitaria, 5000 Córdoba, Argentina*
[3]*CEA, INAC, SP2M, L_sim, 17 rue des Martyrs, 38054 Grenoble Cedex 9, France*
[4]*CIN2 (CSIC-ICN) Barcelona, Campus UAB, E-08193 Bellaterra, Spain*
(Received 12 February 2010; revised manuscript received 14 April 2010; published 7 May 2010)

We report on a theoretical study of charge transport properties of graphene nanoribbons under external mechanical stress. The influence of mechanical forces on the ribbon conductance is shown to be strongly dependent on the ribbon edge symmetry, i.e., zigzag versus armchair. In contrast to zigzag-edge nanoribbons which remain robust against high strain deformations, a stretching-induced metal-semiconductor transition is obtained for armchair-edge configurations. Our results point out that armchair edge ribbons are consequently much better suited for electromechanical applications.

DOI: 10.1103/PhysRevB.81.193404 PACS number(s): 72.80.Vp, 73.22.Pr, 71.30.+h

Once deemed impossible to be found in nature, graphene[1,2] is nowadays considered as one of the most promising materials for the future of electronics at the nanoscale. The rich variety of physical features of graphene includes high carrier mobility,[3] almost perfect crystalline structure, and anomalous quantum hall effect.[4] The expanding horizon of phenomena explored using graphene as a playground includes spintronics,[5] ac transport,[6–8] and thermoelectrics.[9] Moreover, motivated by graphene's lightness and stiffness[10] and the rather flexible electronic character under stress,[11] the interplay between mechanical and electrical properties of graphene became another direction of research beyond the realm of purely electronic or mechanical studies in which such features are the essential functionalities for building up low-cost nanoelectromechanical systems (NEMS) devices.

Recent experimental studies coupling mechanical and electronic degrees of freedom include graphene-based resonators that present low inertial masses, ultrahigh frequencies, and outstanding quality factors even at room temperature.[12–14] Their performance can even overcome those of carbon nanotubes since graphene can offer lower contact resistance. Detailed analysis of the physical properties of uniaxially strained graphene has also been widely studied by Raman spectroscopy.[15,16]

It is clear that the experimental achievements on this field run at a fast pace posing electromechanical graphene nanodevices as a potential reality. However, experiment realizations still face several difficulties that need to be overcome to achieve a full control and development of graphene-based NEMS technology. It is almost impossible for experimental measurements to obtain a pure reaction of graphene sheets under external forces since graphene samples are highly dependent on the surrounding environment. Such challenge surely needs theoretical inputs which can contribute significantly in the understanding of electromechanical response of graphene devices.

At the same time, most of the theoretical counterparts found in the literature are limited to electronic or phononic structures, i.e., not addressing transport issues. For instance, *ab initio* calculations performed in uniaxially strained graphene pointed that their electronic and vibrational band structure features strictly depend on the direction and intensity of the applied strain.[17–19] A lot of recent theoretical efforts has also addressed the large variety of electromechanical effects that could be engineered in two-dimensional graphene including electron beam collimation, confinement, electromechanical sensing capability, and so forth.[20] To date, however, the transport response of graphene nanoribbons under external strain remains to be fully understood.

In this Brief Report, we present a theoretical study of the effects of mechanical forces on the electrical response of graphene nanoribbons. The interplay between mechanical and electrical degrees of freedom on both the electronic structure and the transport properties are explored using a semiempirical method, in which tight binding elements are parametrized from *ab initio* data and conventional Landauer-Büttiker transport formalism. We showed that an energy band-gap engineering is possible when using armchair-edges graphene nanoribbons. In contrast, zigzag-edges ribbons are found to be strongly robust against high strain deformation [as displayed schematically on Fig. 1(a)].

Semiempirical methodology. The adopted approach follows the procedures explained in Ref. 21. Semiempirical potentials constructed from first principles inputs as proposed by Tersoff[22] are implemented to describe the interatomic interactions in hydrocarbon- and carbon-based structures. The potentials are then plugged into Slater-Koster tables[23] to obtain hopping and overlap tight-binding parameters. Strained structures are modeled within static equilibrium approximation in which mechanical forces are applied uniaxially as shown in Fig. 1(a). The total energy of the system plus the mechanical energy resulting from the stretching is minimized with respect to the atomic positions, i.e., $\partial/\partial r(E_T+E_M)=0$. E_T is the total energy computed from the interatomic semiempirical potential, $E_M=-\Delta\vec{\ell}\cdot\vec{F}$, being $\vec{F}$ the external force and $\Delta\ell=\ell-\ell_0$, with ℓ and ℓ_0 the deformed and initial equilibrium lattice constant parameters along the axial direction, respectively. The strain is defined as $\epsilon=\Delta\ell/\ell_0$. The validation of static equilibrium approximation for the particular configurations studied here (armchair and zigzag ribbons) comprehends thresholds of stretching $\epsilon<40\%$ and tempera-

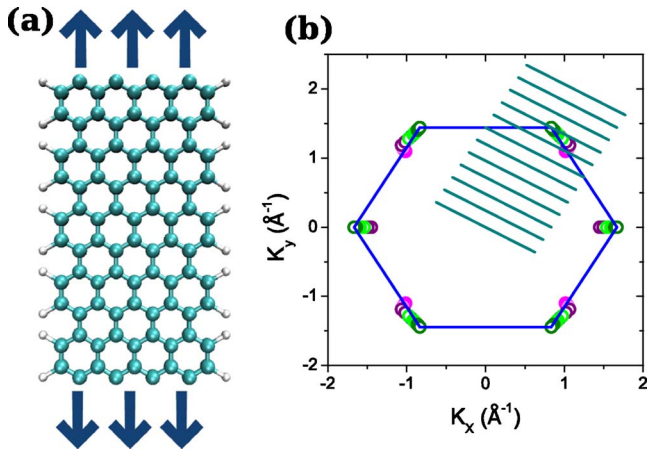

FIG. 1. (Color online) (a) Representation of mechanical uniaxial forces applied on a nanoribbon. (b) Brillouin zone of a graphene and the allowed wave vectors of an AGNRs. Open circles represent the Fermi surface of the ribbon under mechanical stretching.

tures up to 300 K. We confirmed this assumption performing additional molecular dynamics simulations via Velocity-Verlet algorithm.[24] Comparing the atomic configurations obtained from these two approaches, we highlight that the agreement between them within those limits is remarkable.

Finally, the electronic structure of the system is represented by a parametrized third nearest-neighbors tight-binding Hamiltonian. Standard Green's function technique is implemented to resolve band structure and local density of states (LDOS) of relaxed and strained ribbons. Landauer formula[25] is subsequently used to compute the electronic transmission within the coherent transport regime. The electrodes are considered as semi-infinite graphene ribbons which are transparently attached to a central scattering region. The self-energies that describe the influence of the leads are obtained using decimation techniques of the tight binding Hamiltonian. The electronic transmission can be monitored as a function of Fermi energy and stretching forces simultaneously, thereby providing a complete mapping of the interplay between mechanical and electrical properties of pristine nanoribbons.

Effects of mechanical strain. The low-energy properties of monolayer graphene sheets at equilibrium are well represented by two linear energy bands that intersect the high symmetry points of the Brillouin zone (BZ), K and K'. The electronic density of states vanishes linearly at the charge neutrality point, exhibiting a semimetallic behavior. The symmetry of unstrained graphene layers are represented by D_{6h} space point group. However, the number of operations can be markedly reduced under mechanical deformations.[18,19,26–28] This reduction can lead the system symmetry to a simple C_{2h} point group depending on the direction of the pulling.

Nevertheless, even more drastic and fascinating mechanical effects can be revealed for the case of graphene nanoribbons. The symmetry of nanoribbons is represented by the space point group D_{2h} and the width and shape of their edges are crucial elements in determining their electronic and mechanical properties.[29] Novel electrical responses can be thus

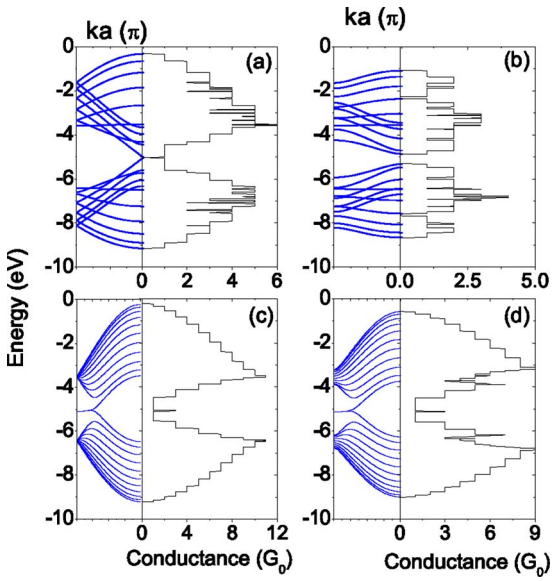

FIG. 2. (Color online) Band structure and conductance for (a) relaxed and (b) strained AGNR-11 with a strain force of 100 nN and (c) relaxed and (d) strained ZGNR-10 with the same strain force.

identified in nanoribbons under stress, which opens new prospects for ultimate nanoelectromechanical resonators. Here, one will only consider zigzag- and armchair-edge symmetries with dangling bonds saturated with hydrogen atoms.

Figure 2 shows a comparison between the relaxed and strained band structures and conductance profiles for a metallic armchair-edge (AGNR) and a zigzag-edge (ZGNR) nanoribbons with N dimers distributed along its width. For the AGNR systems, we state that we are not considering the correction parameter commonly used to model the edge atoms.[30] Therefore, the metallic character can occur in our simulations depending on the width of the ribbon. The relaxed AGNR with $N=11$ presented on panel (a) shows initially a semimetallic behavior and as the uniaxial force is applied, the electronic structure of the system is significantly affected. Indeed, as seen in panel (b), the same ribbon already manifests a semiconducting character with an energy gap of $E_g=0.45$ eV at a mechanical force of $F=100$ nN. We can also notice from the band structures that all the degeneracies at Z point have been lifted under strain. From the point of view of electronic structure, the D_{2h} symmetry of the states remains invariant regardless the amount of mechanical strain. Although the space symmetry group does not change, the pure deformation of the bands is already enough to trigger a strong effect on the transport response of the ribbon. The number of conducting channels is widely reduced within the whole energy range as a consequence of the flatness of the bands under mechanical stress. The same analysis was performed for a ZGNR with $N=10$. It is worth mentioning that spin-polarization effects are not included in our calculations. In this case, a degenerated flat band is formed at Fermi level of ZGNRs. This degeneracy is rather robust and as we learn from our calculations, mechanical strain is not able to split them. Differently from the AGNR geometry, the strain applied to ZGNR does not cause significant changes on their electronic structures as one can see in Figs. 2(c) and 2(d).

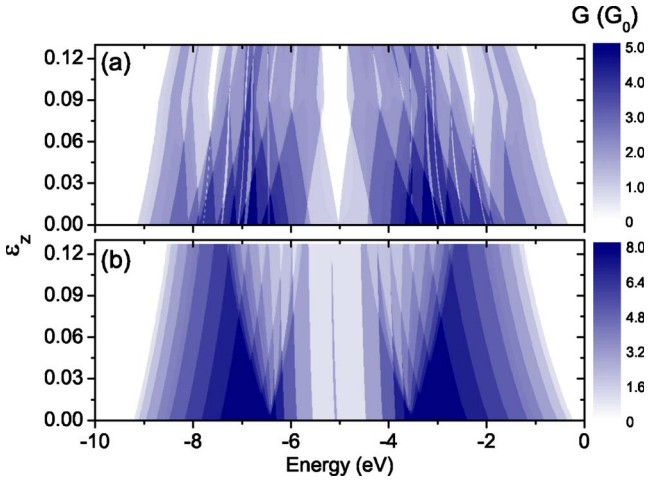

FIG. 3. (Color online) Contour plots of conductance as a function of Fermi energy and mechanical strain for (a) AGNR-11 and (b) ZGNR-10.

The energy dispersion is almost unaltered by mechanical strain. The most affected region is the one in the vicinity of the Z point, where the degeneracy is lifted. In contrast, the degeneracy of the flat bands at the Fermi level is rather robust for even higher mechanical strains. We simply observe a minor deformation on these bands which acquire some dispersion at mechanical force of 100 nN. Moreover, the sorting of the bands remains as those without any stress. This rather insensitivity surely induces small modifications on the transport properties of ZGNRs. In opposite to what AGNRs reveal, no metal-semiconductor transition is observed for ZGNR geometry and the reduction of conducting channels is less remarkable. In other words, ZGNRs can be qualified as unsuitable candidates for building-block components in electric-mechanical nanodevices.

To provide an overall visualization of such electrical-mechanical interplay, we show in Fig. 3 contour plots describing the evolution of the conductance as a function of the Fermi energy and mechanical strain. Results for AGNR-$N=11$ and ZGNR-$N=10$ are, respectively, shown in panel (a) and panel (b). Figure 3(a) shows that very small strain values are able to create an energy gap. In other words, the electronic character of armchair-edge ribbons are rather sensitive to mechanical stress and any small strain can lead the system to a semiconducting behavior. The gap increases almost linearly up to strains of $\epsilon=7\%$, remaining approximately unaffected up to $\epsilon=12\%$, (maximum strain shown in the figure). For mechanical strains higher than 13% (not shown), the band gap diminishes displaying an interesting oscillatory behavior which confirms the tunable features of energy gaps in AGNRs under stretching.[17] Additional gaps are formed in other energy ranges due to the flattening of higher-energy bands. The ZGNR case clearly reflects the robustness of the electronic structure of the ribbon under strain. The degeneracy of the flat bands is slightly lifted only at high loads ($\approx 10\%$) and the number of conducting channels is weakly reduced as the strain increases.

These results highlight the importance of the geometric details of the ribbon when mechanical stress is acting on the system. Different physical responses can be observed depending on the shape of the ribbons. The critical strain value in which an energy gap is opened and the gap size are determined by the edge shape and the width of the ribbons. Combining the feasible ability of tailoring the edge of the ribbons in laboratory with the effects caused by mechanical strain, numerous possibilities of electromechanical devices can be proposed and designed. The fact that they are based on semiempirical framework allows us to extract not only the electronic structure but also the strain-dependent quantum transmission. Even larger systems under strain can be easily treated within this efficient approach that carries the same numerical accuracy as *ab initio* formulations.

Metal-semiconductor transitions observed in AGNRs can be explained tracking the path drawn by the Fermi surface of the ribbon as the stress is enhanced. Figure 1(b) shows the trajectory scratched by K and K' points of a strained AGNR around the two-dimensional BZ of the graphene. One can clearly observe the displacement of the Fermi surface in relation to vertical lines representing the allowed wave vectors of the ribbon. Metal-semiconductor transition induced by strain occurs due to the rearrangement of the electronic orbitals whenever the bonds are stretched. Accordingly, charge transfer is enhanced perpendicularly to the direction of the stretching leading the degenerate point of the bonding and antibonding π bands to move slightly from its original position. In this sense, an energy gap can be closed (opened) depending on the (not) crossing of the vertical lines on the modified Fermi surface. For the ZGNR case, it is straightforward to explain its robustness under stretching. The same BZ picture can be visualized simply changing $k_x \leftrightarrow k_y$. Differently from AGNRs, the set of wave vectors of a ZGNR always lays on K point because the boundary conditions always requires an allowed state at the Γ point, independently of the width of the ribbon. As the amount of strain increases, charge transfer is also enhanced perpendicularly to the stretching direction, deforming the graphene BZ. However, this deformation draws a perfect horizontal track along $k_x=0$ as the strain increases and the degeneracy of the flat bands can never be lifted by mechanical stretching.

Such physical interpretation shares the same ingredients as curvature effects on the electronic properties of carbon nanotubes.[31] Carbon nanotubes can be tailored wrapping a graphene ribbon and a certain amount of mechanical tension is induced along the circumferential direction of the tube. The lattice distortion is even more evident for tubes with smaller diameters (<7 Å) in which the hybridizations of σ and π orbitals are extremely relevant. Single-π band approximation within tight-binding modeling fails to correctly describe the electronic structure of small-diameter nanotubes. In this sense, our model can also be applied to mimic the natural curvature tension of carbon nanotubes without including all the set of atomic orbitals. We can tune the degeneracy points in the BZ via mechanical stretching in such way that they can fit with full *ab initio* calculations. This is a simple and efficient way to extract accurate numerical results in the vicinity of the Fermi energy for small diameter tubes.

Conclusion. We have systematically investigated the role played by mechanical deformations on the transport properties of graphene nanoribbons. Uniaxial forces were simulated

stretching ribbons with armchair- and zigzag-edge shapes. We conclude that armchair-edge ribbons are more suitable for engineering electric-mechanical devices since a metal-semiconductor transition can be monitored with strain deformations. On the other hand, the electronic structure of zigzag-edge graphene nanoribbons is genuinely robust under stretching and no changes on the electronic character are observed in wide range of applied strain. The number of conducting channels is drastically reduced for armchair-edge ribbons whereas the transport response of zigzag geometries is mostly affected for energies around the γ point. Our results overview the main role played by mechanical stretching on the transport properties of the pristine ribbons and will serve as a guideline to interpret more complex mechanical-electrical phenomena at nanoscale.

ACKNOWLEDGMENTS

This work was partially funded by Alexander von Humboldt Foundation, by the WCU (World Class University) program through the Korea Science and Engineering Foundation sponsored by the Ministry of Education, Science and Technology (Project No. R31-2008-000-10100-0), the European Social Funds in Saxony, and the cluster of excellence "ECEMP—European Centre for Emerging Materials and Processes Dresden." We acknowledge the Center for Information Services and High Performance Computing (ZIH) at the Dresden University of Technology for computational resources. S.R. acknowledges the ANR/P3N2009 (project NANOSIM_GRAPHENE Project No. ANR-09-NANO-016-01) and the grant by the Friedrich Willhelm Bessel foundation.

[1] K. S. Novoselov, A. K. Geim, S. V. Morozov, D. Jiang, Y. Zhang, S. V. Dubonos, I. V. Grigorieva, and A. A. Firsov, Science **306**, 666 (2004).
[2] A. H. Castro Neto, *et al.*, Rev. Mod. Phys. **81**, 109 (2009); M. Lemme, Sol. Stat. Phenom. **156-158**, 499 (2010); D. S. L. Abergel *et al.*, Adv. Phys. (to be published).
[3] Y. W. Tan, Y. Zhang, K. Bolotin, Y. Zhao, S. Adam, E. H. Hwang, S. Das Sarma, H. L. Stormer, and P. Kim, Phys. Rev. Lett. **99**, 246803 (2007); A. Lherbier, B. Biel, Y.-M. Niquet, and S. Roche, *ibid.* **100**, 036803 (2008).
[4] K. S. Novoselov *et al.*, Science **315**, 1379 (2007).
[5] Y.-W. Son *et al.*, Nature (London) **444**, 347 (2006); S. Lakshmi, S. Roche, and G. Cuniberti, Phys. Rev. B **80**, 193404 (2009); D. Soriano, F. Muñoz-Rojas, J. Fernández-Rossier, and J. J. Palacios, *ibid.* **102**, 136810 (2009); O. V. Yazyev, Rep. Prog. Phys. **73**, 056501 (2010).
[6] C. Rocha, L. Foa Torres, and G. Cuniberti, Phys. Rev. B **81**, 115435 (2010).
[7] E. Prada, P. Sanjose, and H. Schomerus, Phys. Rev. B **80**, 245414 (2009).
[8] R. Zhu and H. Chen, Appl. Phys. Lett. **95**, 122111 (2009).
[9] Y. M. Zuev, W. Chang, and P. Kim, Phys. Rev. Lett. **102**, 096807 (2009); N. Mingo, K. Esfarjani, D. A. Broido, and D. A. Stewart, Phys. Rev. B **81**, 045408 (2010).
[10] I. W. Frank, D. M. Tanenbaum, A. M. van der Zande, and P. L. McEuen, J. Vac. Sci. Technol. B **25**, 2558 (2007).
[11] Z. H. Ni *et al.*, ACS Nano **2**, 2301 (2008).
[12] J. S. Bunch, A. M. van der Zande, S. S. Verbridge, I. W. Frank, D. M. Tanenbaum, J. M. Parpia, H. G. Craighead, and P. L. McEuen, Science **315**, 490 (2007).
[13] J. T. Robinson, M. Zalalutdinov, J. W. Baldwin, E. S. Snow, Z. Wei, P. Sheehan, and B. H. Houston, Nano Lett. **8**, 3441 (2008).
[14] A. K. Hüttel, G. A. Steele, B. Witkamp, M. Poot, L. P. Kouwenhoven, and H. S. J. van der Zant, Nano Lett. **9**, 2547 (2009).
[15] T. M. G. Mohiuddin *et al.*, Phys. Rev. B **79**, 205433 (2009).
[16] M. Huang *et al.*, Proc. Natl. Acad. Sci. U.S.A. **106**, 7304 (2009).
[17] L. Sun *et al.*, J. Chem. Phys. **129**, 074704 (2008).
[18] M. Mohr, K. Papagelis, J. Maultzsch, and C. Thomsen, Phys. Rev. B **80**, 205410 (2009).
[19] S. Choi, S. Jhi, and Y. Son, Phys. Rev. B **81**, 081407(R) (2010).
[20] V. M. Pereira and A. H. Castro Neto, Phys. Rev. Lett. **103**, 046801 (2009); V. M. Pereira, A. H. Castro Neto, and N. M. R. Peres, Phys. Rev. B **80**, 045401 (2009); O. Hod and G. E. Scuseria, Nano Lett. **9**, 2619 (2009).
[21] D. Porezag, T. Frauenheim, T. Kohler, G. Seifert, and R. Kaschner, Phys. Rev. B **51**, 12947 (1995).
[22] J. Tersoff, Phys. Rev. Lett. **56**, 632 (1986); Phys. Rev. B **37**, 6991 (1988); Phys. Rev. Lett. **61**, 2879 (1988).
[23] J. C. Slater and G. F. Koster, Phys. Rev. **94**, 1498 (1954).
[24] W. C. Swope *et al.*, J. Chem. Phys. **76**, 637 (1982).
[25] M. Buongiorno Nardelli, Phys. Rev. B **60**, 7828 (1999); F. Triozon, Ph. Lambin, and S. Roche, Nanotechnology **16**, 230 (2005).
[26] L. Yang and J. Han, Phys. Rev. Lett. **85**, 154 (2000).
[27] K. S. Nagapriya, S. Berber, T. Cohen-Karni, L. Segev, O. Srur-Lavi, D. Tomanek, and E. Joselevich, Phys. Rev. B **78**, 165417 (2008).
[28] T. Cohen-Karni *et al.*, Nat. Nanotechnol. **1**, 36 (2006).
[29] A. Cresti *et al.*, Nano Res. **1**, 361 (2008).
[30] M. Ezawa, Phys. Rev. B **73**, 045432 (2006).
[31] J.-C. Charlier, X. Blase, and S. Roche, Rev. Mod. Phys. **79**, 677 (2007).